ELSEVIER

Journal of Structural Geology 26 (2004) 1755–1772

JOURNAL OF STRUCTURAL GEOLOGY

www.elsevier.com/locate/jsg

Evidence for non-plane strain flattening along the Moine thrust, Loch Srath nan Aisinnin, North-West Scotland

Matthew Strine*, Steven F. Wojtal

Department of Geology, Oberlin College, Oberlin, OH 44074-1044, USA

Received 23 May 2003; received in revised form 15 January 2004; accepted 24 February 2004

Available online 13 May 2004

Abstract

We report quartz *c*-axis patterns, grain-shape fabrics, and microstructures for 11 mylonitic quartzites and quartz-phyllosilicate schists from a transect across the Moine thrust at Loch Srath nan Aisinnin, North-West Scotland. In the footwall samples collected more than 42 m normal distance from the thrust surface, quartz *c*-axis textures indicate a general flattening strain (i.e. $0 < k < 1$). Samples within 19 m normal distance of the thrust are completely recrystallized and exhibit asymmetric *c*-axis patterns. Recrystallized hanging wall fault rocks exhibit random *c*-axis patterns on the scale of a standard thin section.

Relict footwall grains provide the closest approximation of finite strain; they have octahedral shear strains (ϵ_s) between 1.10 and 1.47 and exhibit general flattening *k*-values (0.0524–0.659). The long axis of the mean relict grain shape trends parallel to the regional transport direction and plunges gently to the ESE. In contrast, recrystallized footwall grains have a mean grain shape with the longest axis oriented nearly perpendicular to the transport direction. Furthermore, these samples have grain shape *k*-value ranges from 0.157 to 0.295. Recrystallized hanging wall grain shapes exhibit the lowest octahedral shear 'strains' ($\epsilon_s = 0.532–0.733$) and largest mean *k*-values (0.351–0.961) of this sample set. The long axes of the mean recrystallized hanging wall grain shapes are parallel to transport, similar to that of relict footwall grains. Unrecrystallized quartz overgrowths about opaque mineral grains suggest concurrent elongation in all directions within the mylonitic foliation and support the inference of general flattening deformation.

The mylonitic foliation and penetrative lineation are consistent with a WNW shearing direction; however, both were folded during later deformation increments. Recrystallized grains in footwall quartzites suggest a 305–320° azimuth for the shearing direction. The best-fit π-axis of the poles to the foliation is 18,145, close to the mean trend/plunge of mesoscopic fold hinges at this site (18,151). Both suggest a NNW azimuth for the shearing direction. Thus, structural, microstructural and fabric indicators suggest a change in the azimuth of the shearing direction from ~286 to ~331°.

Keywords: c-Axes; Fold–thrust belts; Grain shape analysis; Kinematics; Moine; Mylonites; Non-plane strain; North-West Scotland; Preferred orientation; X-ray goniometry

1. Introduction

Most fold-and-thrust belts are arcuate in nature, giving rise to a pattern of large-scale salients and recesses (Marshak, 1988; Lawton et al., 1997; Mitra, 1997). Similarly, individual thrust faults have arcuate traces in map view (above and beyond the effect of interaction with an irregular surface topography) suggesting that thrust faults, in general, have non-planar geometries (Dahlstrom, 1970; Elliott and Johnson, 1980; Boyer and Elliott, 1982). Three-dimensional complexities in the shapes of individual thrust faults and in the overall configuration of fold-and-thrust belts lead to three-dimensional variations in the velocity and displacement fields within thrust sheets and, thus, in the distribution of incremental and finite strains within those sheets. Lateral changes in macroscopic geometry of thrust-related structures and documented non-plane strains at the mesoscopic and microscopic scales (e.g. Durney and Ramsay, 1973; Ramsay and Huber, 1983; Geiser, 1988; Mukul and Mitra, 1998; Twiss and Unruh, 1998) attest to the three-dimensional nature of displacement fields within thrust sheets. Moreover, variations in material behavior over space and time also contribute to the

* Corresponding author. Present address: Department of Earth and Environmental Sciences, University of Rochester, Rochester, NY 14627, USA. Tel.: +1-585-275-5713; fax: +1-585-244-5689.

E-mail address: matty@earth.rochester.edu (M. Strine).

0191-8141/$ - see front matter © 2004 Elsevier Ltd. All rights reserved.
doi:10.1016/j.jsg.2004.02.011

three-dimensional variations in displacement and strain fields within individual thrust sheets and across fold-and-thrust belts (Hossack, 1967; Coward and Kim, 1981; Sanderson, 1982; Mitra, 1997; Gray and Mitra, 1999). In the face of these complexities, current mechanical models fail to predict realistic fold-and-thrust belt behavior, except at the largest scale. The most widely accepted mechanical models of fold-and-thrust belt behavior (e.g. critical taper models of Chapple (1978), Davis et al. (1983), Emerman and Turcotte (1983) and Fletcher (1989)) are based on assumptions of plane strain and spatially and temporally uniform material behavior. Likewise, most computational models used to examine the kinematic or mechanical development of structures associated with thrust emplacement (e.g. Smart et al., 1997, 1999; Strayer and Hudleston, 1997, 1998) treat thrust faults as planar or smoothly curved surfaces above which rocks undergo plane strain deformation. In order to develop better models of the kinematic and dynamic evolution of fold-and-thrust belts, we need a more complete understanding of the three-dimensional geometry and the associated incremental deformation history of these belts.

We report data from quartz-rich, thrust-related mylonites from a transect across the Moine thrust near Loch Srath nan Aisinnin (Fig. 1). The transect crosses the Moine thrust within a prominent recess along the fault trace produced by a local steepening of the thrust surface (Elliott and Johnson, 1980). Field measurements of fold hinge, foliation, and lineation orientations were compiled from this area. We examined our samples petrographically, measured crystallographic preferred orientations in quartzites and quartz-rich layers of schists, and measured the three-dimensional shapes of both relict and recrystallized quartz grains. Together, these data indicate that at this location along the Moine thrust non-plane strain deformation dominated, strongly non-coaxial deformation prevailed within a zone at least 9 m thick, and that the shearing direction may have changed by more than 40° during the thrust's history.

Thrust zone structures and microstructures at the Stack of Glencoul, where the Moine thrust has a shallower dip, indicate that strongly non-coaxial deformation was confined to a layer about 30 cm thick adjacent to the thrust surface within the footwall and lack any evidence for a change in shearing direction (Law et al., 1986; Law, 1987, 1990). The Stack of Glencoul is less than 7 km to the south of the transect we describe here. Combining data from both locations suggests that the local geometry of a thrust surface has a strong influence on thrust zone kinematics. Three-dimensional irregularities of small and large size occur along most thrust surfaces. What are their effects on the overall kinematics and mechanics of thrust systems? This contribution endeavors to identify how irregularities affect the emplacement of individual thrust sheets and begins to assess how irregularities in fault surfaces affect the overall evolution of fold-and-thrust belts.

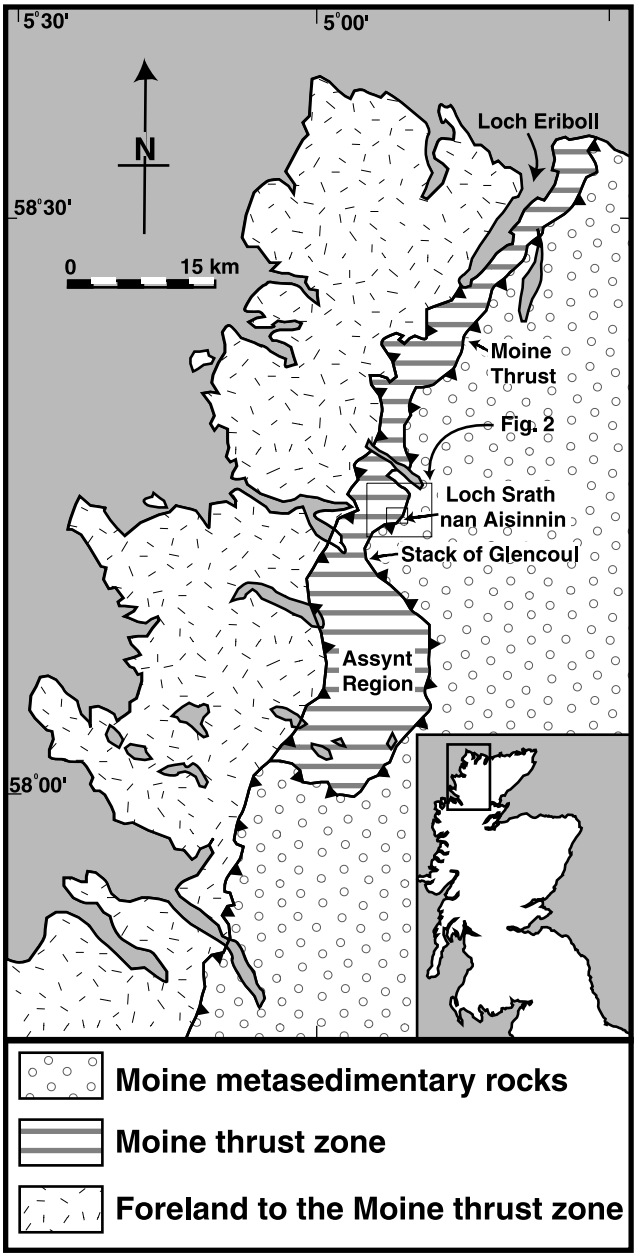

Fig. 1. Sketch map of northern Scotland modified from Law et al. (1986) showing the location of the Moine thrust zone, the trace of the Moine thrust, and the location of the study area (small box).

2. Geologic setting

2.1. The Moine thrust zone, North-West Scotland

The Moine thrust zone is a NNE-striking, ESE-dipping series of thrusts of which the Moine thrust is the easternmost and oldest (Peach et al., 1907; Elliott and Johnson, 1980; Coward, 1988). The Moine thrust extends along strike at least 190 km from the Point of Sleat in the south to Whiten Head on the coast of Sutherland (Peach et al., 1907; Christie, 1963) (Fig. 1). It carried Proterozoic, quartzofeldspathic, Moine metasedimentary rocks to the WNW,

over Archean age Lewisian gneisses, late Proterozoic age Toridonian sandstone, and Cambrian–Ordovician quartzites and limestones (Peach et al., 1907; Elliott and Johnson, 1980; Coward, 1988). Most workers define the azimuth of sheet movement to be parallel to the trend of the penetrative lineation in extensively deformed rocks within the thrust zone, i.e. 290–295° (Cloos, 1946; Coward et al., 1992). Displacement magnitudes are difficult to determine for the Moine thrust, and a large range of values has been suggested. Elliott and Johnson (1980) estimated a minimum displacement of 75 km from their balanced cross-sections.

The Moine and associated thrusts formed during the Caledonian orogeny. Plastic deformation within the Moine thrust zone occurred from 443–435 Ma to approximately 430 Ma (van Breemen et al., 1979; Johnson et al., 1985; Kelley, 1988; Freeman et al., 1998; Dallmeyer et al., 2001). The Moine thrust belt was tilted 8–12° to the ESE during post-orogenic extension (Elliott and Johnson, 1980). Owing to this tilting, erosion has exposed structures formed at relatively deep crustal levels. For this reason, and due to its classic geometry, the Moine thrust belt has been studied by generations of geologists as a type example of large-scale thrusting.

A mylonite layer 0–70 m thick developed adjacent to the Moine thrust during thrusting (Peach et al., 1907; Christie, 1960, 1963; Evans and White, 1984). Thrust-related mylonites exhibit a greenschist facies mineral assemblage (Johnson et al., 1985; Kelley and Powell, 1985; Harris and Johnson, 1991; Freeman et al., 1998). Regional metamorphic isograds in calc–silicate rocks of the Moine metasediments also tend to parallel the trace of the Moine thrust, with metamorphic grades increasing eastward (Johnson, 1983). Both the mylonitic foliation within the Moine thrust zone and the foliation in the Moine schists just above the thrust zone are parallel to the thrust surface (Christie, 1963). Farther from the thrust surface, within the Moine thrust sheet, the dip of foliation varies by as much as 20°. Folds are very common within the mylonites. The amplitudes of folds tend to increase with distance from the thrust surface. Many of these have sheath fold geometries (Carreras et al., 1977; Evans and White, 1984; Holdsworth, 1990; Alsop and Holdsworth, 1999). Christie (1963) documents fold axes that plunge gently to the ESE (~100°), subparallel to the inferred regional transport direction.

Near the midpoint of its map trace, the emplacement of a series of footwall imbricates folded the Moine thrust into a broad, doubly-plunging antiform. At the center of this antiform, called the Assynt culmination, the Moine thrust has an elevation more than 1 km higher than at other locations along strike (Elliott and Johnson, 1980). North of the Assynt culmination is located a similar but much smaller structure that also created a recess within the map trace of the Moine thrust (Figs. 1 and 2). It is within this smaller structure, north of Loch Srath nan Aisinnin, that the samples described in this paper were collected.

2.2. The Moine thrust zone near Loch Srath nan Aisinnin

Loch Srath nan Aisinnin is located approximately 15 km northeast of the Assynt culmination, approximately midway between the well-known Moine thrust localities at Loch More and the Stack of Glencoul (Figs. 1 and 2). This segment of the Moine, which generally dips 10–20° to the ESE, places mylonitized Moine metasedimentary rocks against mylonitic quartzites of the Pipe-rock and Basal Quartzites (Peach et al., 1907; Butler, 1984). The penetrative lineation is inclined shallowly to the ESE, nearly down the dip of the prominent primary foliation in these rocks (Fig. 2). Mesoscopic folds in both hanging wall and footwall rocks fold this lineation, indicating that the fold hinges in this area are oblique to it. In fact, the vector mean of fold hinges plunges to the SSE, and both foliations and lineations vary in orientation due to this later folding. The best-fit π-axis of poles to foliation also plunges SSE, only ~8° from the vector mean fold hinge orientation (Fig. 2). Immediately adjacent to the thrust surface, folds have wavelengths and amplitudes of millimeters to several centimeters and cause only minor reorientation of the penetrative lineation. More than a few meters from the thrust surface in both the hanging wall and the footwall, fold wavelengths and amplitudes are several tens of centimeters to a few meters, and the reorientation of the penetrative lineation is distinctive. Neither the base nor the top of the thrust zone in this segment is planar, so the thickness of mylonitized Moine metasediments and footwall quartzites varies along strike. Southwest of Loch Srath nan Aisinnin, the Moine mylonites thin abruptly, leading to an abrupt change in the orientation of the schistosity in the overlying Moine schists. In addition, one well-defined kink locally reorients the thrust surface, and the adjacent footwall quartzite and hanging wall quartzschist. We infer that this fold formed after the main phase of ductile shearing had ceased possibly during late stage out-of-sequence reactivation of the Moine thrust (Butler, 1984; Coward, 1988; Holdsworth, 1989).

We collected 11 samples along the north side of Loch Srath nan Aisinnin, where a thick layer of Moine schist mylonites has been emplaced above Cambrian Basal Quartzite (Figs. 1 and 2). These samples can be categorized into three main groups. Our first group consists of five samples collected from the footwall at map distances ranging from 154 to 512 m from the fault trace and normal distances >42 m below the thrust. All of these samples have deformed relict quartz grains. The next group consists of three footwall samples collected close to the thrust (map distances <72 m and normal distances 19–0 m from the thrust surface). These samples have been thoroughly recrystallized such that original grain boundaries cannot be recognized. The last group consists of three hanging wall samples, all within 50 m map distance from the fault trace. The quartz layers from within these samples have also been totally recrystallized.

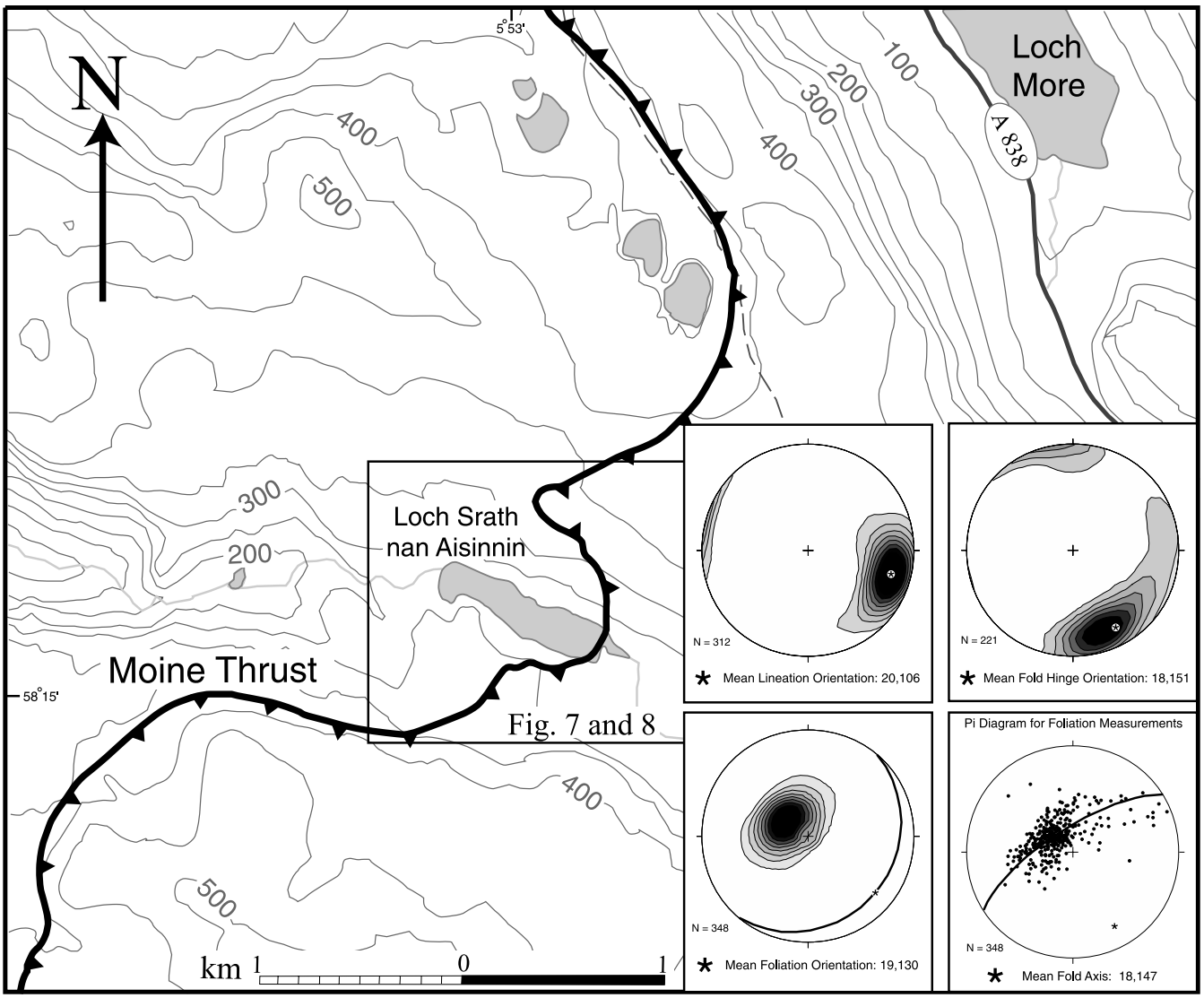

Fig. 2. Generalized topographic map of sample area near Loch Srath nan Aisinnin and field data collected from this area. Data plotted using Richard Allmendinger's StereoNet program, Version 4.9.6. Vector means are calculated as described in text.

3. Methods

Three mutually perpendicular sections were cut from each sample for petrographic analysis: one perpendicular to both the lineation and the mylonitic foliation (*a*-section), one parallel to the lineation and normal to the mylonitic foliation (*b*-section), and one parallel to the mylonitic foliation (*c*-section) (Fig. 3). We undertook standard petrographic analyses of these sections, and cataloged the occurrence of different microstructures, such as undulose extinction, deformation lamellae, deformation bands, etc. in quartz-rich layers in these rocks.

Quartz *c*-axis data were primarily collected using an optical microscope and a universal stage. For each of the samples, we measured an equal number of *c*-axes from each of the three perpendicular thin sections (most commonly 100 grains per thin section). For the five footwall samples that have relict quartz grains preserved, the *c*-axes were

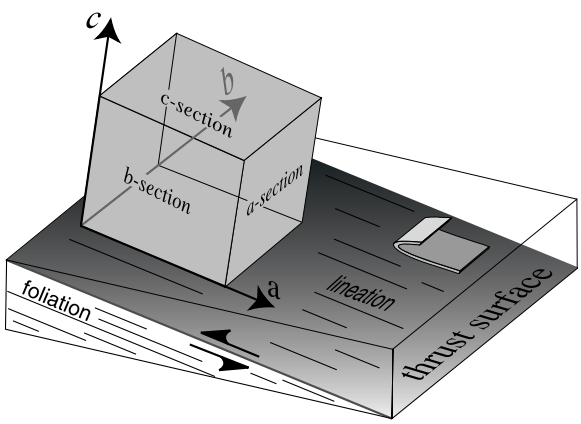

Fig. 3. Illustration of terminology used to describe the kinematic reference frame and orientation of thin-sections.

measured exclusively from relict grains. For the rest of the samples, *c*-axes were measured from recrystallized quartz grains. Holger Stunitz at the University of Basel, Switzerland, kindly collected quartz *c*-axis data via X-ray goniometry to verify our optical measurements for seven of our 11 samples. All these data were rotated and plotted on lower hemisphere equal-area projections such that the foliation is vertical and oriented 'left–right', and the lineation is horizontal.

We also calculated vector mean values for lineations, poles to foliations, fold hinge lines, and grain shape approximation axes. Since most stereonet programs use downward directed vectors to represent linear data, we got unreasonable values when using these programs to calculate vector means. For any line, there are two vectors that can be chosen to represent it, and the vector one chooses will have an effect on the vector mean. For instance, lines 000,05 and 180,07 clearly should have an average orientation of 180,01, but programs that use downward directed vectors to represent these two lines calculate a vector mean of 000,89. Therefore, we calculated our vector means by first 'eye-balling' a vector mean approximation and then choosing the vector that is oriented fewer than 90° from this estimated value to denote each individual linear orientation. It is from these vectors that our vector means were calculated.

Finally, we determined the mean shapes of quartz grains (both relict and recrystallized grains) using the R_f/ϕ method. We approximated cross-sections through grains as ellipses and measured their axial ratio, R_f, and orientation defined by the angle, ϕ, relative to the trace of foliation in *a*- and *b*-sections or relative to the lineation in the case of *c*-sections. The axial ratios were measured optically using graduated cross-hairs, and determined ϕ by stage rotation. Borradaile (1984) showed that measuring 50–75 elliptical strain markers is sufficient to constrain an accurate strain measurement and that additional measurements do not significantly increase the precision of the data. Thus, we felt confident measuring 100 grains per thin-section to determine our two-dimensional elliptical grain shape approximations. From these raw data, harmonic and vector means were calculated using the method outlined by Lisle (1985). The data was collected from three mutually perpendicular thin sections per sample. These data were then used to determine the best-fit ellipsoid using a Mathematica program developed by Strine (http://www.earth.rochester.edu/structure/matty/3-D_Strain_Program_page/Strain_Program_page.html), which essentially takes a least squared approach. In this method, the measured axial ratio and angular orientation data are subtracted from the axial ratio and angular orientation of a general ellipsoid defined in terms of six unknown matrix elements. The differences are squared and summed, and this sum is then minimized to calculate the best-fit values for the matrix elements and hence the best-fit ellipsoid. The program then rotates the best-fit ellipsoids into their geographic reference frame and gives the trend and plunge of the three principal axes as well as their axial ratios and associated *k*-values.

4. Character of deformation in the Moine thrust zone at Loch Srath nan Aisinnin

4.1. Deformation microstructures

Footwall Cambrian quartzite samples collected between 154 and 512 m from the fault trace at Loch Srath nan Aisinnin consist of coarse, highly deformed relict grains within a much finer recrystallized quartz matrix (Fig. 4a). All five of these samples have a well-defined foliation and mineral lineation. The mylonitic foliation is defined by the long and intermediate axes of the deformed relict grains as well as thin (approximately 20 μm) layers of white mica around the relict grains. This foliation is locally perturbed by minor asymmetric crenulations (Fig. 4b). Relict grains exhibit a mantling of subgrains around their grain boundaries. The interiors of the grains are highly undulose and/or have deformation bands. The fine-grained matrix grains have polygonal boundaries and exhibit uniform extinction, implying low dislocation densities.

Recrystallized footwall quartzite samples from the Moine thrust zone (found within 19 m normal distance from the thrust surface) at Loch Srath nan Aisinnin are nearly monomineralic, consisting almost entirely of fine-grained quartz. These quartzites exhibit prominent mylonitic banding, Sa, parallel to the thrust and a penetrative ESE-plunging lineation evident in outcrop and hand sample. In both *a*- and *b*-sections, the mylonitic banding is apparent as millimeter-thick layers of slightly coarser- and finer-grained quartz (Fig. 4c). Quartz grains within individual layers sometimes extinguish uniformly. Many grains exhibit undulose extinction, suggesting moderate dislocation densities. Distinct grains are separated by irregular to polygonal grain boundaries. We infer that this microstructure developed by dynamic recrystallization of quartz. The average diameter of recrystallized grains in each sample is approximately 25 μm. Recrystallized quartz exhibits a dimensional preferred orientation oblique to the mylonitic banding, Sa, defining a secondary foliation, Sb. The angle between Sa and Sb ranges from 40 to 50° within the *b*-sections (Fig. 4c). The relatively high angle between Sa and Sb may be due to an approximately horizontally directed shear strain component; however, it is important to keep in mind that these recrystallized grain shapes do not represent strain in the traditional sense. Within the *b*-sections of quartzite mylonites adjacent to the thrust surface (sample F-1), irregular, lens-shaped domains of coarse-grained quartz give evidence for relict detrital grains and/or relict veins. These domains are also evident in *a*-sections, although with less extreme axial ratios when compared with those in the *b*-sections. We infer that the quartz domains are attenuated relict grains and/or rotated veins that have a flattened-ribbon shape. These elongate relict grain shapes and/or rotated veins imply significant crystal plastic deformation. In *c*-sections, the elliptical to lens-shaped regions of coarse-grained quartz define the lineation. Small

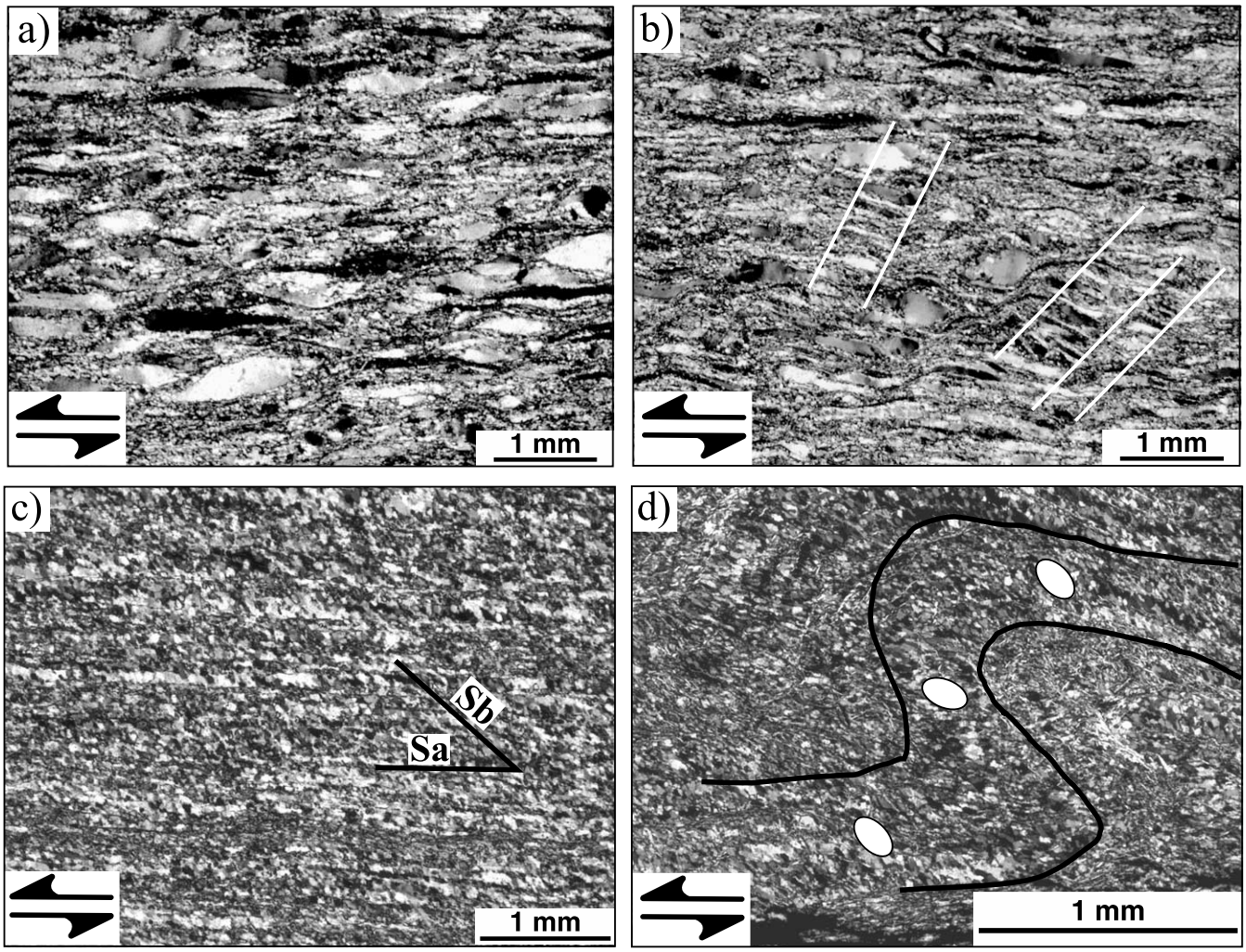

Fig. 4. Crossed nicols photomicrographs of deformed footwall quartzites. All images are taken from the *b*-section with the bottom of the photographs parallel to the penetrative lineation, viewed to the NNE. (a) Deformed relict grains, (b) Kinked relict grains. White lines outline kink bands. (c) Sa–Sb fabric within recrystallized footwall quartzite. Banding visible as millimeter-thick layers of slightly coarser- and finer-grained quartz. Note uniform to slightly undulose extinction, and irregular to polygonal boundaries. (d) Asymmetric fold of phyllosilicate-rich and quartz-rich layers from a recrystallized footwall sample with the recrystallized grain fabric consistent with flexural slip folding.

grains of white mica are disseminated throughout individual bands of fine-grained quartz. These mica flakes are aligned with the mylonitic foliation in *a*- and *b*-sections and with the lineation in *c*-sections, but they are rarely abundant enough to impart a fissility to the rock. In sample F-3, very thin, often discontinuous layers of fine-grained white mica occur along the margins of some bands. Especially where mica layers are relatively thick, the mylonitic layering is commonly folded (Fig. 4d). Folds are common in *b*-sections and less distinct in *a*-sections; undulations of layering in *c*-sections support the inference that fold hinges are curved and folds are non-cylindrical. The geometry of the recrystallized quartz grains around the folds is consistent with the strains patterns expected in flexural folds and therefore recrystallization must have been synchronous with folding (Fig. 4d).

Pelitic Moine schists adjacent to the thrust surface are finely laminated, with alternating quartz-rich and phyllosilicate-rich layers. Quartz-rich layers resemble individual bands in the mylonitic Basal Quartzite, i.e. they are composed mainly of fine quartz grains separated by irregular to polygonal grain boundaries (Fig. 5a). Quartz extinguishes uniformly or, at most, exhibits moderate undulose extinction. Here, too, recrystallized quartz exhibits a prominent grain-shape fabric that defines a secondary foliation, Sb, oblique to the mylonitic banding, Sa, but at a lower angle than that seen in the footwall (Figs. 4c and 5a). Numerous opaque grains (probably magnetite) have short, fibrous quartz overgrowths in both the *a* and *b* directions. Only rarely are fibers still recognizable at distances greater than ~1.2 times the diameter of the opaque grains. Typically, quartz surrounding opaque grains is so thoroughly recrystallized that its origin is obscured. Phyllosilicate layers contain chlorite, muscovite, and phlogopite grains aligned parallel or at a very low angle to the lamination. Some phyllosilicate layers are nearly planar and extend across an

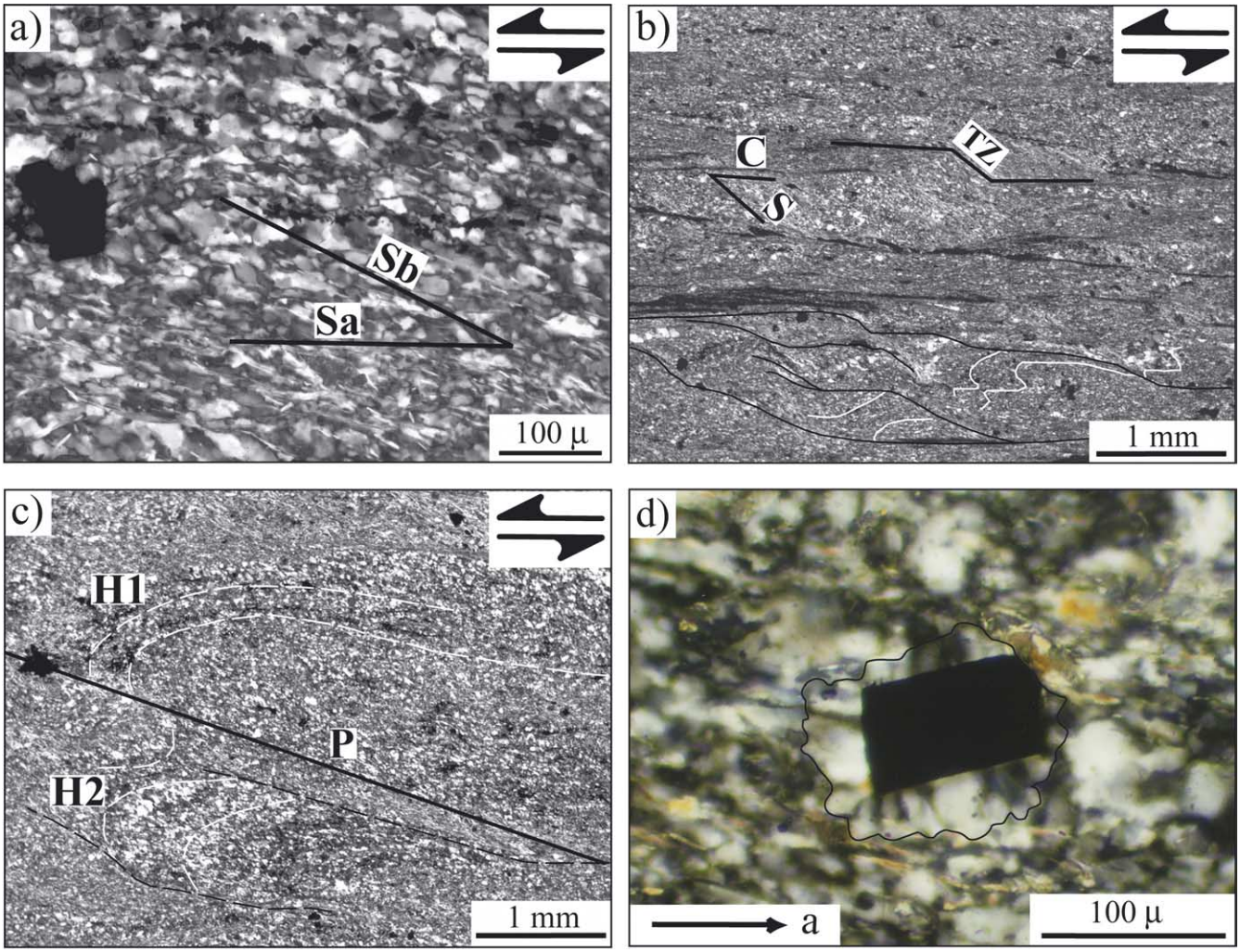

Fig. 5. Crossed nicols photomicrographs of deformed hanging wall Moine schists. All images save (d) were taken from *b*-sections with the bottom of the photographs parallel to the *a*-direction, viewed to the NNE. (a) Sa–Sb fabric in a quartz-rich layer. (b) S–C fabric defined by thin phyllosilicate layers (S) oriented obliquely to the mylonitic banding (C), which is defined by nearly continuous and planar phyllosilicate layers extending across the field of view. Near the center of the field of view there is a step or 'transfer zone' within the phyllosilicate-rich layer (TZ). White line delineates some intra-folial folds. (c) Millimeter-scale intra-folial folds outlined by dashed white lines. Note adjacent antiformal hinges (H1 and H2) separated by a segment of phyllosilicate-rich layer (P, highlighted by the solid black line). (d) Radial quartz overgrowths on an opaque grain (probably magnetite) in the *c*-section.

individual thin section. Both diffuse distributions of small phyllosilicate flakes and local concentrations of phyllosilicates oriented obliquely to these planar phyllosilicate layers define a foliation oriented approximately 45° to the planar phyllosilicate layers. We interpret these two elements as defining an S–C fabric (Berthé et al., 1979) in the rock (Fig. 5b). Phyllosilicate layers may also possess steps ('transfer zones') or end in 'horsetails' (see figs. 8 and 9 in Boyer, 1984) (Fig. 5b). At some locations in phyllosilicate layers, individual grains are kinked or oriented at high angles to the lamination, and neighboring grains exhibit different orientations. The attitudes of phyllosilicate grains in these locations suggest small slip surfaces and folds within individual phyllosilicate layers. In fact, in most *b*-sections and in some *a*-sections truncated, asymmetric, intra-folial folds occur between nearly planar phyllosilicate layers (Fig. 5c). In *c*-sections, layering appears wavy, suggesting that fold hinges are curved and folds are non-cylindrical. Judging from the waviness of layers in *c*-sections, the curvature of fold hinges is much less than the curvature of layers observed in *a*- or *b*-sections. In the vicinity of Loch Srath nan Aisinnin, folding is ubiquitous in the Moine schist mylonites. Here, in contrast to what Christie (1963) and Evans and White (1984) reported for other segments of the Moine thrust, most fold hinges plunge fairly consistently to the SSE in outcrop and in hand sample, oblique to the prominent lineation in the mylonitized rocks (Strine and Mitra, 2004) (Fig. 2).

Rocks farther above the thrust surface exhibit different microstructures. First, the quartz-rich layers have a larger amount of phyllosilicate minerals and have a less uniform microstructure farther from the thrust surface. Quartz-rich layers contain very fine-grained quartz (with grain diameters <10 μm) together with the more typical 20–25 μm

diameter recrystallized grains. Quartz grains range from uniformly extinguishing to strongly undulose; most have irregular grain boundaries. Isolated large quartz grains or aggregates of coarse quartz occur in most layers. In some cases, these large quartz grains or quartz aggregates are partially replaced by calcite or dolomite. These large quartz grains exhibit strongly undulose extinction, and often possess prominent polygonal subgrains. Quartz grains in coarse aggregates have polygonal grain boundaries and exhibit uniform extinction. Most quartz-rich layers also contain numerous small chlorite grains aligned oblique to layering, small equant to rounded grains of opaque minerals, epidote, other minor minerals (sphene, apatite, etc.), and feldspar grains of a range of sizes. Quartz or quartz-chlorite overgrowths parallel to the *a* and *b* directions occur on some opaque grains and minor minerals, but many grains lack overgrowths. Phyllosilicate-rich layers are also less regular in mineral composition, thickness, and orientation when compared with phyllosilicate layers in rocks closer to the thrust surface. At some locations, phyllosilicate-rich layers are 50–75 μm thick and composed almost entirely of chlorite. At others, thin phyllosilicate layers are mixtures of chlorite, white mica, and quartz. In the latter, phyllosilicate grains are strongly aligned parallel to layering. In the former, phyllosilicate grains are not always strongly oriented. Non-cylindrical, intra-folial folds sandwiched between planar, phyllosilicate-rich layers and asymmetric, non-cylindrical folds of quartz-rich and phyllosilicate-rich layers are common in these rocks.

4.2. Deformation mechanisms and kinematics

The five footwall samples, all of which contain relict grains, have microstructures that indicate large crystal plastic strains. The relict grains show considerable elongation in both the *a* and *b* sections. Matrix grains and the margins of relict grains are strongly recrystallized. Due to the non-equant grain shapes, the existence of subgrains, and the lack of bulging grain boundaries, we interpret this material to have been recrystallized via subgrain rotation. Both the core and mantle structure and the dominance of subgrain rotation recrystallization are consistent with Regime 2 type deformation conditions (Hirth and Tullis, 1992). The asymmetry of the shapes and the orientations of the relict grains as well as the sense of asymmetry of the crenulations are consistent with a WNW sense of shearing (Fig. 4b). The short limbs of crenulations are aligned along kink bands dipping between 35 and 60° to the WNW. One sample (F-7) has kink bands that dip shallowly (between 15 and 20°) to the WNW. This sample also records a significantly higher amount of flattening when compared with the other four samples.

In the three quartzite samples collected closest to the thrust surface at Loch Srath nan Aisinnin, microstructures associated with early stages of mylonitization have been obscured by extensive recrystallization. Still, the shape, size, and orientation of these recrystallized grains hold some clues to deformation in this area. The microstructures in the quartzites near the thrust surface (i.e. the layers of uniformly to moderately undulatory extinguishing, fine-grained quartz separated by irregular to polygonal grain boundaries, and the dimensional preferred orientation of new grains oblique to the mylonitic foliation within the quartz-rich layers) are interpreted as being the product of extensive recrystallization. Microstructurally, it is difficult to assess whether these samples deformed under Regime 2 or Regime 3 conditions (Hirth and Tullis, 1992). Due to the small grain size and existence of quartz overgrowths in the adjacent hanging wall, diffusive mass transfer probably also contributed to the deformation of these rocks. The well-defined fabrics of elongate subgrains and recrystallized grains oblique to the mylonitic banding in these rocks are consistent with top-to-the-WNW shearing (Means, 1981; Simpson and Schmid, 1983; Dell'Angelo and Tullis, 1989; Ree, 1991). The mylonitic layering has been folded on the scale of millimeters; folds are particularly common adjacent to relatively thick mica-rich layers.

Microstructures in quartz-rich domains in the mylonites derived from Moine schists suggest that they too have recrystallized via subgrain rotation. Elongate grains in quartz-rich layers and the S–C fabrics, transfer zones, and horsetails in the phyllosilicate-rich layers in these rocks are also consistent with top-to-the-WNW shearing. Fibrous quartz overgrowths on opaque minerals and other rigid grains in these rocks provide direct evidence for diffusive mass transfer of quartz and chlorite. Overgrowths are clearest in *b*-sections, but they are also visible in *a*- and *c*-sections. In *c*-sections, overgrowths can be seen to define a radial pattern, with the longest fibers parallel to the *a*-direction (Fig. 5d). The radial overgrowths are consistent with non-plane strain flattening deformation. The overgrowths are themselves partially recrystallized, indicating that dynamic recrystallization either took place during or after fiber growth. Farther from the thrust surface, overgrowths are not as thoroughly recrystallized.

In Moine mylonites, some quartz-rich domains appear to have originated as quartz veins. They are now nearly parallel to the mylonitic foliation. Both the mylonitic layering and the early quartz veins are typically folded on a millimeter scale. This folding may have been facilitated by the alternation of quartz-rich and phyllosilicate-rich layers, which contributes to anisotropy in these fault rocks.

Within 10 m of the thrust surface, fault rocks derived from Moine schists lack biotite; chlorite is the primary ferromagnesian mineral, thus recording greenschist facies conditions. With increasing distance above the thrust, rocks contain progressively more biotite and less chlorite, suggesting that the mineral assemblages within 10 m of the thrust surface have been altered by retrograde metamorphism (Knipe and Wintsch, 1985). Feldspar porphyroclasts decrease in size and abundance in samples successively closer to the fault. This decrease in feldspar

is accompanied by an increase in white mica. This transition from feldspar-rich to mica-rich mineral assemblages is typical of ductile deformation zones within quartzo-feldspathic rocks material when water is present (Mitra, 1978; Knipe and Wintsch, 1985).

4.3. Quartz c-axis data

Owing to the predominance of dislocation creep microstructures, we were encouraged to measure crystallographic preferred orientations for quartz in these rocks. Quartz mylonites adjacent to the thrust surface exhibit an asymmetric kinked single girdle (Sample F-1, Fig. 6). Sample F-2, approximately 9 m normal distance from the thrust surface, also has a strong single girdle pattern (Fig. 6). By 19 m normal distance from the thrust (sample F-3), the strongly asymmetric *c*-axis pattern is gone (Fig. 6). In sample F-3, the *c*-axis pattern resembles a broken, asymmetric Type I (Lister, 1977) crossed girdle with a large concentration of axes plotted in the center of the stereoplot (i.e. subparallel to the *b*-direction, normal to the *b*-section; Fig. 3). Still farther below the thrust surface, between 154 and 512 m map distance (and more than 42 m normal distance) from the fault trace, the *c*-axis texture changes again. All five samples from this segment of our transect across the thrust zone have a broken symmetric cross girdle (samples F-8–F-4; Fig. 6). Each pattern lacks *c*-axes in the center of the girdle (i.e. subparallel to the *b*-direction), and the two samples closer to the fault (F-4 and F-5) approach a small circle girdle centered about the *c*-direction (i.e. the pole to the foliation) (Fig. 3).

Polymineralic rocks generally partition strain unevenly among their constituent minerals (Handy, 1990). Such inhomogeneity may cause complex flow patterns that militate against the development of well-defined crystallographic preferred orientations. In fact, crystallographic textures in polymineralic rocks are often much weaker than those in monomineralic rocks (e.g. Tullis and Wenk, 1994) and may be too weak to be meaningful (e.g. Starkey and Cutforth, 1978). Still, Dell'Angelo and Tullis (1986) showed that experimentally deformed aplites had similar quartz *c*-axis patterns to comparably deformed quartzite. Further, White et al. (1982) found no difference between the quartz *c*-axis patterns measured in quartz-rich layers and

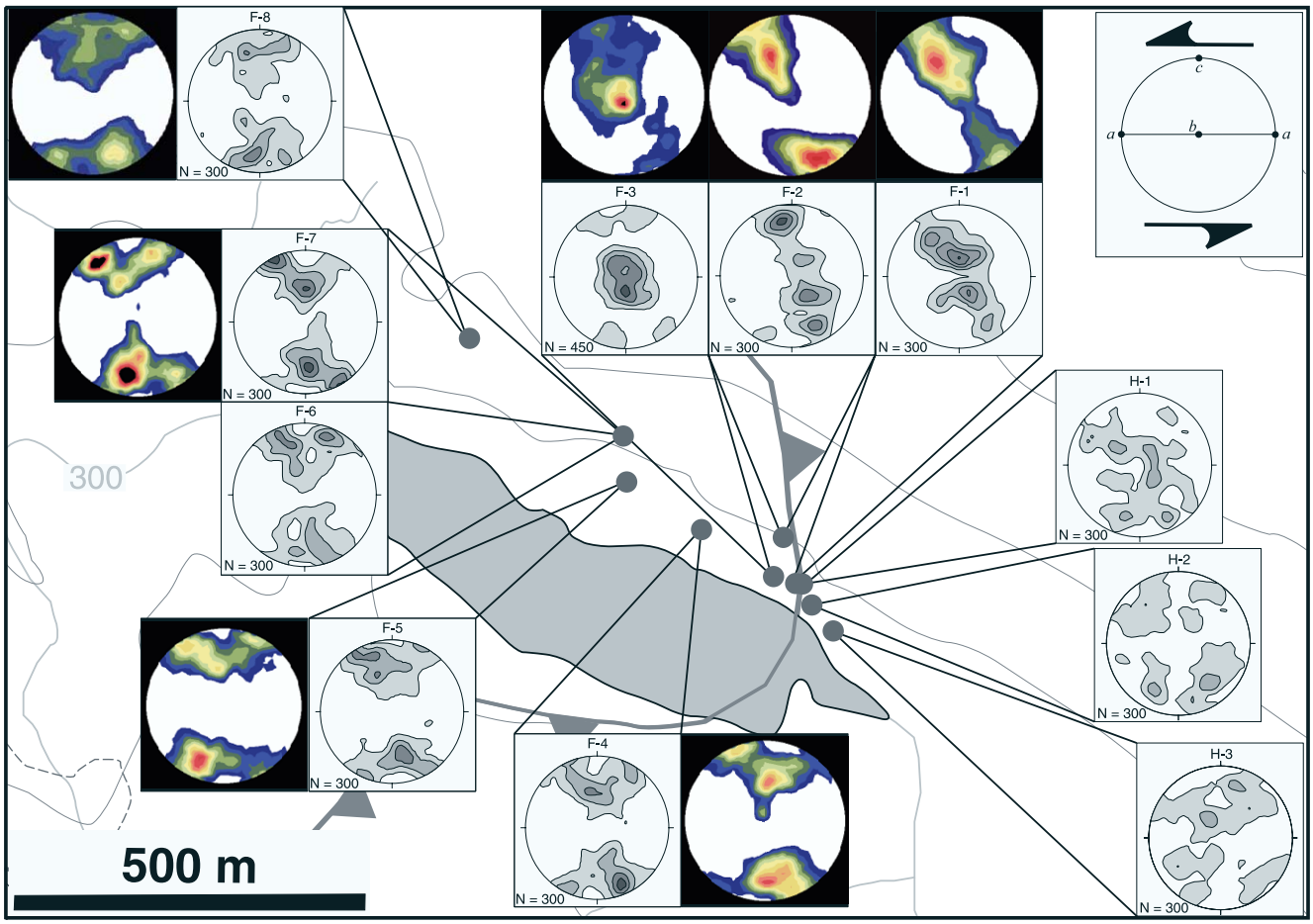

Fig. 6. Site map showing both optically measured (white bordered) and X-ray goniometry (black bordered) quartz *c*-axis data. Plots are all equal-area lower hemisphere projections viewed toward the NNE. Foliation is vertical and oriented left–right and lineation is horizontal. Contour intervals are consecutive multiples of a uniform distribution.

quartz-phyllosilicate layers from the Moine thrust zone, and Law et al. (1984) found well-defined crystallographic preferred orientations for quartz domains in sheared quartz schists. For these reasons, we decided to investigate the crystallographic preferred orientations in recrystallized quartz-rich layers in mylonitized Moine schists (samples H-1–H-3). On the scale of a standard thin-section, however, randomly sampled quartz grains in these samples showed weak to random *c*-axis textures (Fig. 6).

4.4. Grain shape fabrics

We determined three-dimensional grain shapes by measuring the mean elliptical shapes and orientations (via the R_f/ϕ method) from three mutually perpendicular thin sections per sample and then calculating a best-fit ellipsoid. Fig. 7 shows the location, shape, and orientation of the determined grain shape ellipsoids. The grain shape data can most easily be evaluated on the Flinn plot in Fig. 8 (Flinn, 1962). A Flinn plot is useful because it simultaneously gives information about the grain shape (i.e. where the data plot in relationship to the two extremes of pan-cake shaped, $k = 0$, and cigar shaped, $k = \infty$) and 'strain magnitude' (here shown in terms of octahedral shear strain, ϵ_s; Nadai, 1963, p. 73). One should note that we have plotted values for recrystallized grain shapes on the same Flinn diagram as the relict grains. The shapes of recrystallized grains do not yield information on finite strains; nevertheless, they are useful kinematic indicators. The data plotted in Fig. 8 show that all the samples have *k*-values less than one, i.e. they fall within the general flattening deformation field. Although there is overlap between the ranges of *k*-values between the three groups of samples defined above, each group has a distinctive mean value (k_{av}): relict footwall grains $k_{av} = 0.351$, recrystallized footwall grains $k_{av} = 0.237$, and recrystallized hanging wall grains $k_{av} = 0.609$. Moreover, the three groups exhibit distinct ranges in ϵ_s. For relict footwall grains $\epsilon_s = 1.10–1.47$, recrystallized footwall grains have $\epsilon_s = 0.787–0.937$, and recrystallized hanging wall grains show $\epsilon_s = 0.532–0.733$). Thus, in 'Flinn-space' the three groups plot within distinct regions.

A different pattern emerges in the orientations of the long, intermediate, and short axes of the grain shape ellipsoids. The mean long axes of relict footwall grains and recrystallized hanging wall grains plunge shallowly to the ESE, subparallel to the macroscopic lineation and the regional transport direction (cf. Figs. 2 and 9). Also, these grains both have subhorizontal mean intermediate axis

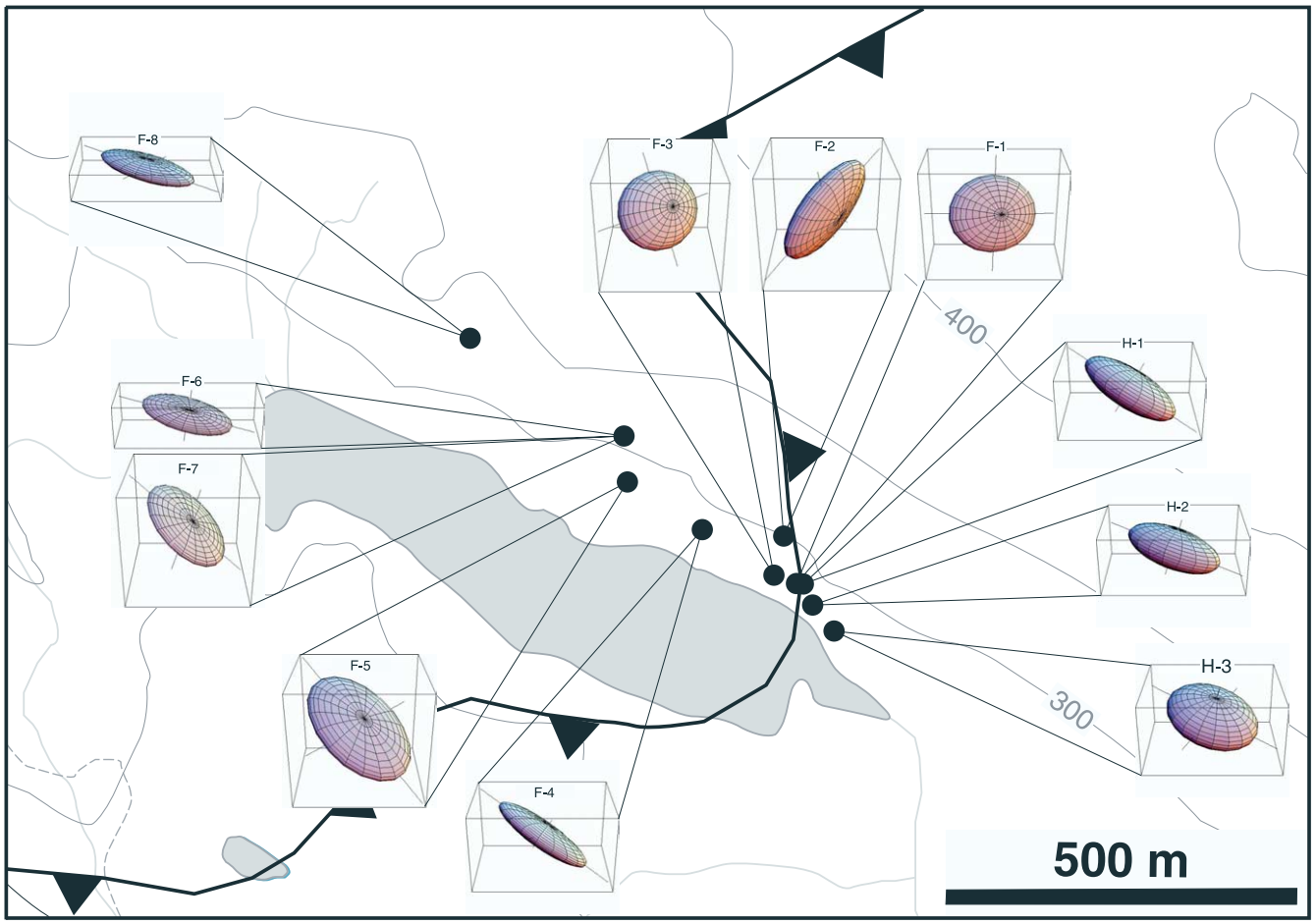

Fig. 7. Site map showing the spatial distribution of ellipsoidal grain shapes plotted with respect to the geographic reference frame.

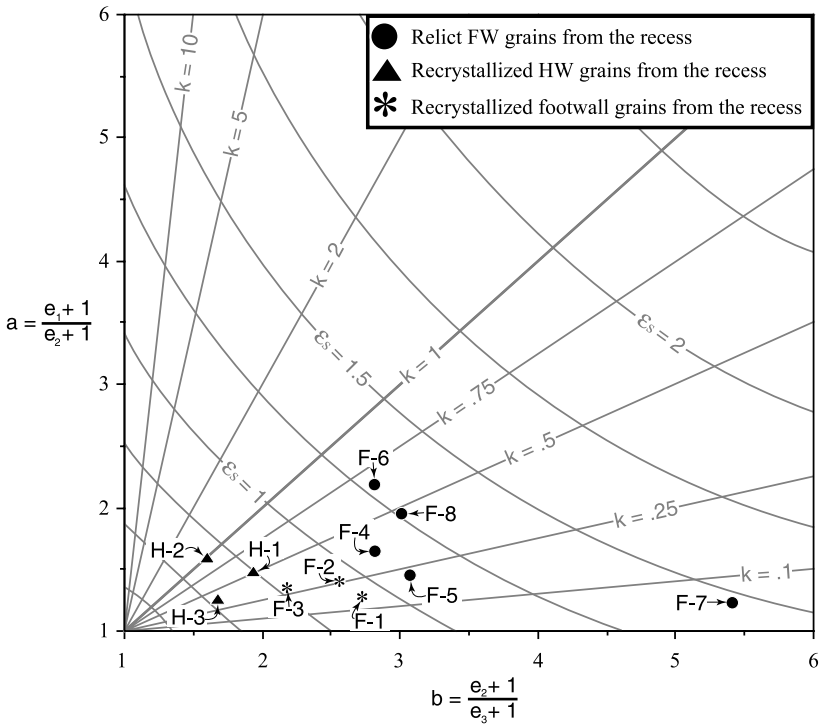

Fig. 8. Grain shape data plotted on a Flinn diagram with calculated k-value and Nadai strain magnitude, ϵ_s, contours (Flinn, 1962; Nadai, 1963).

orientations trending NNE–SSW, and steeply plunging mean short axis orientations. In contrast, recrystallized footwall grains have their long axes oriented perpendicular to the regional transport direction trending NE–SW, steeply plunging intermediate axes and shallowly plunging short axes (Fig. 9).

5. Discussion

5.1. Interpreting quartz c-axes patterns

Crystallographic preferred orientations (CPO) are relatively faithful and robust records of deformation kinematics (Ree and Park, 1997). Although they do not give quantitative information on strain magnitudes, CPOs yield insight into strain geometry and symmetry. In the footwall at Loch Srath nan Aisinnin, the k-values of inferred strains are consistent with the c-axis patterns for deformed relict grains. The c-axis patterns for the recrystallized footwall grains, however, do *not* conform with their grain shapes, which are controlled by incremental strains. We infer, therefore, that the crystallographic preferred orientations integrate the effects of deformation over relatively long time intervals. To the extent that one can infer incremental strain geometries from recrystallized grain shapes, the latest deformation increment (where the maximum extension direction is parallel to the b-direction) does not match the earlier deformation increments, here inferred from c-axis textures that were not significantly altered by the last stage of deformation (and therefore give evidence for a simple shear dominated deformation).

As noted above, quartzites with relict footwall grains (samples F-8–F-4) exhibit c-axis patterns that resemble a broken cross girdle, with two of the patterns nearly small circle girdles. The symmetry of the c-axis textures implies an orthorhombic strain symmetry. A fully formed cross girdle is generally thought to imply plane strain deformation, $k = 1$, and a small circle girdle implies pure flattening, $k = 0$, centered about the direction of shortening (Passchier and Trouw, 1996, pp. 92–95). A hybrid, somewhere between these two patterns, would imply a general flattening deformation (i.e. $0 < k < 1$). Thus, we interpret the c-axis patterns in samples F-8 to F-4 to indicate general flattening strains. For comparison, quartzites more than 30 cm below the Moine thrust at the Stack of Glencoul (just 7 km SSW of Loch Srath nan Aisinnin; Fig. 1) exhibit fully symmetrical Type I (Lister, 1977) crossed girdle patterns (Law et al., 1986; Law, 1987) (Fig. 10). Typically, such Type I cross-girdle c-axis patterns (e.g. samples SG.3 and SG.10 in Fig. 10) would be interpreted as being the result of plane strain ($k = 1$; Flinn, 1962) pure shear deformation. However, Law (1987) interprets the X-ray goniometry data from sample SG.10 for both a- and c-axes to be consistent with a general flattening deformation (i.e. $0 < k < 1$). Furthermore, the relict grain strain data from this sample yields a k-value of 0.05 (Schmid and Casey, 1986), supporting an inference of non-plane flattening. The kinked single girdle c-axis pattern seen in samples F-1 and F-2 (at 0 and 9 m normal distance from the thrust surface, respectively) is consistent with essentially simple shear

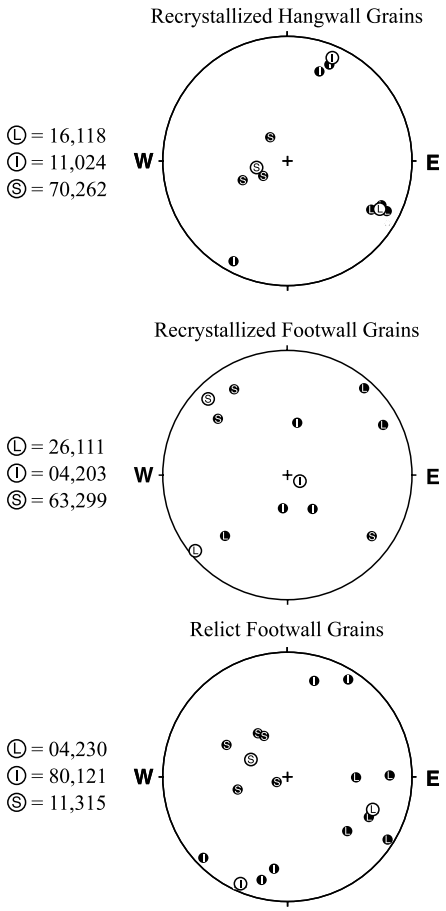

Fig. 9. Lower hemisphere, equal area plots of grain axis orientations and calculated mean orientations. L = Long axis, I = Intermediate axis, and S = Short axis. Individual data points are black circles while the mean values are white circles. Vector means are calculated as described in text.

deformation with a top-to-the-WNW shear sense and suggests a monoclinic strain symmetry (White et al., 1982; Law et al., 1984, 1986; Law, 1987). Quartz *c*-axis data for quartz mylonites within 30 cm of the Moine thrust at the Stack of Glencoul exposure likewise exhibit asymmetric, single-kinked girdle patterns (Law et al., 1986; Law, 1987).

Law et al. (1986) reported asymmetric *c*-axis patterns near the thrust surface and an increase in symmetry with increasing distance from the thrust surface at the Stack of Glencoul, a pattern suggesting that non-coaxial simple shear dominated along the thrust surface and that coaxial deformation dominated away from the thrust. Our Loch Srath nan Aisinnin transect indicates a comparable transition from apparent plane strain simple shear to flattening but also reveals significant differences from the pattern reported by Law et al. (1986) and Law (1987). At the Stack of Glencoul, fully symmetric *c*-axis textures are observed in samples as close as 30 cm normal distance from the thrust surface (sample SG.3, Fig. 10) (Law, 1987), whereas at Loch Srath nan Aisinnin the asymmetric, single-kinked girdle pattern persists up to 9 m below the thrust. Moreover the form of the symmetric *c*-axis pattern differs between these to locations. At the Stack of Glencoul, the symmetric *c*-axis patterns form a Type I (Lister, 1977) crossed-girdle (e.g. samples SG.3 and SG.10, Fig. 10) (Law, 1987), whereas at Loch Srath nan Aisinnin the symmetric textures are a hybrid of a small circle girdle and a crossed-girdle. Furthermore, at Loch Srath nan Aisinnin, as the *c*-axis texture starts to approach a symmetric pattern at 19 m below the thrust (sample F-3) there is a conspicuous concentration of axes subparallel to the *b*-direction. Tullis and Heilbronner (2002) reported a similar 'Y-parallel' (*b*-parallel using our terminology) *c*-axis texture in quartzites deformed experimentally under Hirth and Tullis (1992) Regime 3 deformation conditions. Moreover, microstructures in all three of the recrystallized footwall rocks are consistent with an inference of deformation under Regime 3 conditions, although, it is difficult to demonstrate an increase in grain boundary migration. Thus, the differences seen in *c*-axis patterns within these three samples appear to be the result of a decrease in magnitude of simple shear deformation away from the thrust. Again, this observation is consistent with the data reported by Law et al. (1986) and Law (1987) with the notable difference that the transition from simple shear dominated *c*-axis textures to pure shear dominated texture takes place considerably farther below the thrust. The change from Regime 2 to Regime 3 fabrics suggests a decrease in flow stress, usually accommodated by an increase in temperature or a decrease in strain rate. An increase in temperature is possible when thrusting a relatively hot sheet of rock onto a cooler footwall. However, a decrease in flow stress could be achieved through the

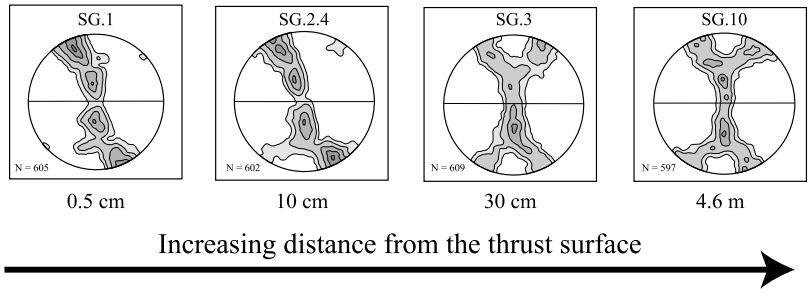

Fig. 10. Quartz *c*-axis data from the Stack of Glencoul taken from Law et al. (1986). Distance from the thrust surface is indicated beneath each lower hemisphere equal area projection. All projections viewed toward the NNE. Foliation is vertical and oriented left–right, and lineation is horizontal.

alignment of easy-glide planes. In such a case, there could be a shift from Regime 2 to Regime 3, which is *not* a result of an increase in temperature or decrease in strain rate but simply extensive recrystallization that aligned glide planes.

The combination of orthorhombic and monoclinic strain symmetry yields an overall monoclinic symmetry for this area owing to the shared symmetry plane (the *b*-plane; Fig. 3). Such symmetry of deformation elements is consistent with deformation patterns observed in many other thrust zones (cf. Law et al., 1984, 1986; Wojtal, 1986; Law, 1987; Twiss et al., 1991, Twiss and Unruh, 1998; Wojtal, 2001). Regime 3 textures, high-strain microstructures, as well as the relatively large distance the asymmetric textures penetrate into the underlying footwall, suggest that the footwall in this area underwent a higher degree of deformation than in the adjoining salient, where random textures occur within 50 m map distance from the fault trace (Strine and Mitra, 2004). Variations in fault-zone character over distances (measured along the fault surface) of a few kilometers are common (Wojtal and Mitra, 1988; Woodward et al., 1988; Erickson and Wiltschko, 1991; Newman and Mitra, 1993), suggesting that the detailed kinematics of fault-zone deformation can change abruptly along strike as well as up and/or down the dip of a thrust.

Quartz mylonites from the three hanging wall Moine schist samples exhibit weak to random *c*-axis textures. *c*-Axis patterns may have developed during deformation, but we believe that they were obscured by the development of thrust-related folds. The Moine schist mylonites have an abundance of millimeter- to centimeter-scale folds (Christie, 1963; Evans and White, 1984). We envision, like many other workers (e.g. Carreras et al., 1977; Cobbold and Quinquas, 1980; LaTour, 1981; Evans and White, 1984; Hanmer and Passchier, 1991; Passchier and Trouw, 1996; Casey and Williams, 2000; Hongin and Hippert, 2001), that transposition associated with continued shearing eventually returns the layering within the rock to an orientation similar to its pre-folding state. As folds initiate, are kinematically amplified, and are eventually transposed into a new mylonitic foliation, *c*-axis textures will be continually reoriented by folding. Furthermore, millimeter-scale folding causes local strain inhomogeneities at a scale smaller than a thin-section. Since recrystallization is synchronous with folding, *c*-axis textures will likely reflect the strain patterns of individual folds (Law, 1990). Consequently, *c*-axis patterns in rocks with ubiquitous small-scale folds are only useful when examined on the scale of the individual folds.

5.2. Interpreting grain shape fabrics

Deformed relict grains preserve the largest part of the deformation history and thus yield the largest strain values (ϵ_s from 1.1 to 1.47) (Fig. 8). One should note that the recrystallization of relict grains around their grain boundaries undoubtedly introduces some error into the strain measurements of these grains. In footwall samples with relict grains, the three-dimensional grain shapes suggest a general flattening strain, which is consistent with the *c*-axis textures (Fig. 10). One sample (F-7) exhibits a low *k*-value of 0.0524. This is the only sample with shallowly dipping kink bands (measured from the *b*-section). We suggest that it has experienced large flattening strains due to some localized strain inhomogeneity. The long axes of the relict grains trend ESE, consistent with WNW directed thrusting. Moreover, the intermediate axes lie within the foliation plane parallel to the regional vorticity axis (i.e. perpendicular to the transport/shear direction).

For comparison, other authors have reported strain ratios on the order of 1:3.5 and 1:2 (in the *b*-section) in the non-mylonitized tectonites associated with the Moine thrust at Loch Eriboll and the Stack of Glencoul (McLeish (1971) and Law et al. (1986), respectively) (Fig. 1). McLeish (1971) calculated strain ratios of approximately 1:10 from sheared *Skolithus* burrows in mylonites derived from the Pipe-rock directly adjacent to the thrust at the Stack of Glencoul (Fig. 1). Wilkinson et al. (1975) calculated shear strains of $\gamma \sim 10$ from similar *Skolithus* tubes. Christie (1963) measured axial ratios on the order of 1:10:100 for relict quartz grains in footwall mylonites in the Assynt region (Fig. 1).

In strongly recrystallized fault rocks, including those from the Moine thrust zone, recrystallized grain shapes must be interpreted with caution. The secondary foliation, Sb, oblique to the mylonitic foliation is interpreted as being a steady-state foliation and is by definition insensitive to the finite strain state (Means, 1981; Ree, 1991). Although the particular microstructures in recrystallized tectonites may have any one of several precursory grain boundary geometries (Means and Ree, 1988), the shapes of recrystallized grains, even in steady-state foliations, preserve information on incremental strains (see figs. 1 and 9 in Ree, 1991). For this reason, we infer that the three-dimensional shapes of recrystallized quartz grains provide some clues to incremental strains in the thrust zone, and thus, give us a unique insight into the last increment of deformation.

The recrystallized footwall grains have shapes indicating a general flattening deformation ranging from 0.157 to 0.295. However, these grains are oriented with their long axes perpendicular to the regional transport direction (Fig. 9). It is possible to have the direction of maximum elongation perpendicular to the shearing direction with monoclinic deformation; in fact, the direction of maximum elongation may switch from parallel to normal to the shear direction as strain accrues (Tikoff and Greene, 1997). Such a switch in lineation orientation is predicted by modeling of transpressional strain (Sanderson and Marchini, 1984; Fossen and Tikoff, 1993; Robin and Cruden, 1994) and results when a relatively small amount of coaxial pure shear is added to a primarily simple shear deformation (Fig. 11). The pure shear component has such a dramatic effect on the strain geometry of dominantly non-coaxial deformation because each successive increment of coaxial pure shear

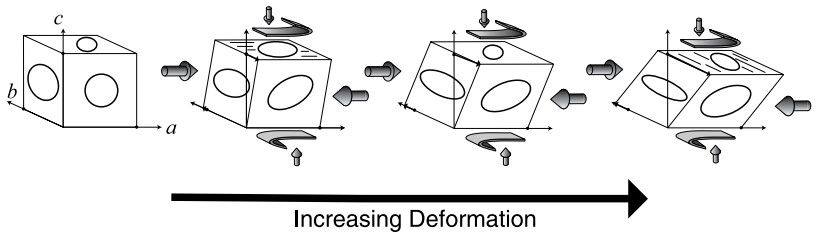

Fig. 11. Strain resulting from the addition of coaxial pure shear extension parallel to the *b*-direction (as a result of the addition of vertical and horizontal flattening, along the *c*- and *a*-directions, respectively) to a horizontal shear zone (dominated by simple shear) through progressive deformation. The maximum extension direction switches with increased deformation. Modified from Tikoff and Greene (1997).

extension has the same orientation, whereas the simple shear extension direction is continually changing. Thus, each increment of pure shear further reinforces the previous increments, which has a major effect on the shapes of grains even for small proportions of pure shear.

In fault rocks from the hanging wall, recrystallized quartz grains have orientations similar to the relict footwall grains and substantially different from recrystallized grains in the adjacent footwall (Fig. 9). This pattern may indicate that the thrust marks a strong discontinuity in deformation kinematics, or it may indicate that hanging wall quartz grains experienced different strains due to strain partitioning among the various minerals within the pelitic Moine schists. The recrystallized hanging wall grains also have *k*-values less than one, consistent with the radial overgrowths seen surrounding opaque grains (Fig. 5d). The hanging wall grains are further distinguished because they have the lowest strain, ϵ_s, and the largest *k*-values.

We argued above that the finite strain data *and* the quartz *c*-axis data integrate the effects of numerous deformation increments, whereas the shapes of recrystallized grains reflect only the latest deformation. We also noted that fabric elements in the thrust-related mylonites at Loch Srath nan Aisinnin display overall a monoclinic symmetry. At Loch Srath nan Aisinnin, the mean shearing direction obtained from the relict footwall grains (294°) and the recrystallized hanging wall grains (285°) is consistent with the transport direction inferred from the mean lineation direction (283°), the transport direction estimated by Coward et al. (1992) (290–295°) and the shearing direction inferred from Christie's (1963) fold axes measurements (~280°) (Fig. 2). The mean shearing directions given above were calculated by averaging the shearing direction inferred from each of the three axes (e.g. for the relict footwall grains: ((111 + 180) + (203 + 90) + (299))/3) (Fig. 9). However, the shearing direction obtained from the recrystallized footwall grains is more northerly (309). The mean orientation for the axes of minor folds at this location is 18,151 (suggesting a shearing direction of 331°), and the π-axis for poles to foliation is 18,145 (with an implied shearing direction of 325°) (Fig. 2). These sheath-like folds reorient the mylonitic foliation and lineation, implying that they are a later stage feature. If they are true sheath folds, their geometry indicates a late stage NNW shearing direction. The recrystallized grains in the footwall suggest an azimuth for the shearing direction that is intermediate between that inferred from the relict footwall grains and that suggested by the late folds. These data are interpreted as recording a change in the flow direction during the final stages of deformation in this region. The finite strain approximations recorded in the relict grains would be relatively insensitive to a late shift in flow direction due to the high strain values that they record.

It is possible that the bulk kinematics is consistent with monoclinic symmetry although fabric elements are perturbed by the development of folds, slip surfaces, etc. In this scenario, the lack of an exact match in the shearing directions measured in different footwall samples would reflect expected scatter about a mean shearing direction. Alternatively, a discrepancy between the two sets of data may indicate that the bulk kinematics of the fault zone varied with time. If this is the appropriate way to interpret these data then the recrystallized grains suggest a temporal change in azimuth of the shearing direction from ~290 to ~309°. In such a scenario, the orientations of the late folds visible in outcrop would be nearly parallel to the shearing direction. Since the recrystallized grains record a later increment of strain, they are consistent with a clockwise rotation in the overall flow direction as observed by the SSE plunging fold axes. Finally, it may be possible that the mylonites in the Loch Srath nan Aisinnin segment of the Moine thrust developed within a general, triclinic shear zone (Lin et al., 1998; Lin and Jiang, 2001).

5.3. Kinematic model

Our preferred model for the deformation in the region of Loch Srath nan Aisinnin consists of a combination of nearly thrust-normal flattening and thrust-parallel shearing. The predominance of general flattening strains over plane strain simple shear and pure shear is not expected in thrust zones. Nevertheless, McLeish (1971), Law et al. (1984), and Law (1987) all found evidence for local flattening along the Moine thrust. One explanation for the non-plane flattening is the development of a footwall imbricate stack. Butler (1984) documented the existence of footwall imbricates in this area. Continued regional shortening against an imbricate stack could give rise to non-plane flow as the major

thrust sheet is forced to flow around the obstruction (Fig. 12). This model assumes that movement continued along the Moine thrust during the development of the footwall imbricate stack. The mylonites in the vicinity of Loch Srath nan Aisinnin occur along a minor recess in the trace of the Moine thrust (Fig. 1). As documented in the Assynt region, a recess along the Moine thrust can occur where a stack of footwall imbricates folds the thrust and raises the Moine sheet (Elliott and Johnson, 1980). The latter hypothesis may also explain why deformation kinematics in the vicinity of Loch Srath nan Aisinnin differ so significantly from those determined at the Stack of Glencoul, less than 7 km away (Law et al., 1986; Law, 1987). The Stack of Glencoul occurs along a minor salient of the Moine thrust, not within a recess (Fig. 1).

The question remains, "why do salients and recesses of this kind form, and why is the deformation between these areas so different?" We suggest that within salients, owing to their shallower dip, deformation is primarily accommodated by slip along the fault and the associated shear, whereas within the recess, where the fault has been steepened, there is less slip and more internal deformation (Fig. 12). The difficult question to answer is what initiates the geometric differences seen between salients and recesses of this kind. The internal deformation seen in the recess may develop as a positive feedback loop. In other words, if, for

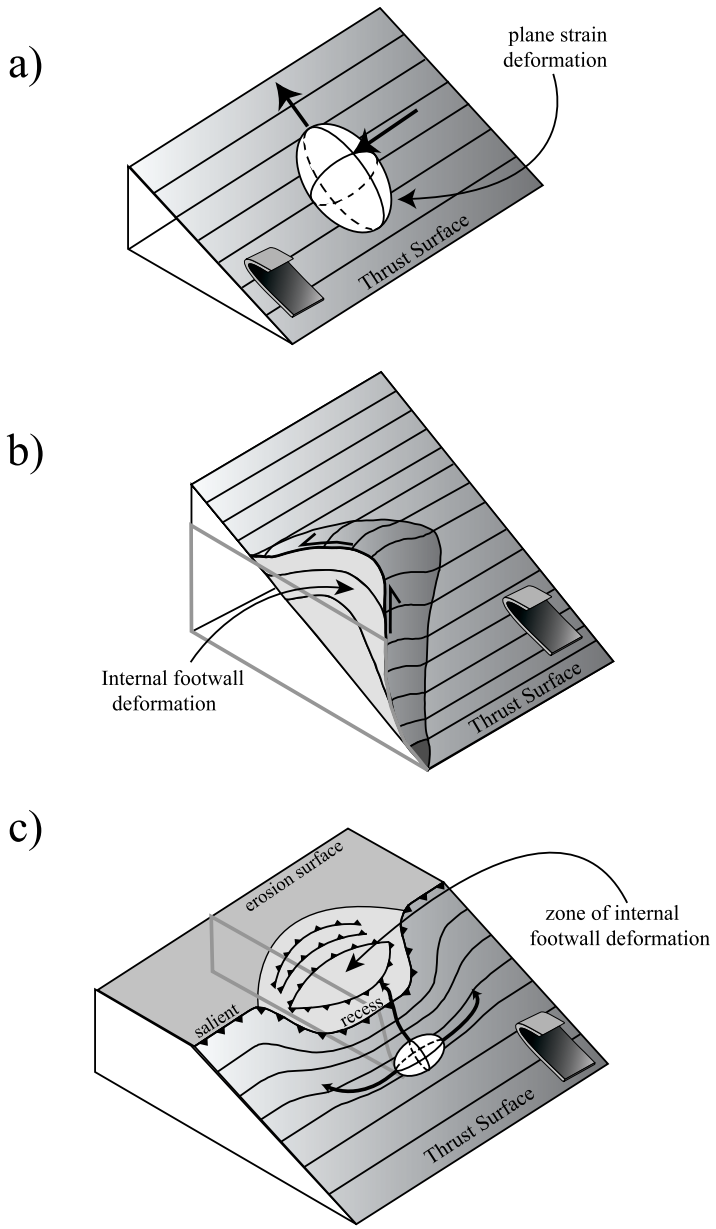

Fig. 12. Schematic diagram showing the possible kinematic implications of footwall deformation. (a) Simple footwall ramp undergoing plane strain deformation. (b) Shape of the distorted thrust surface after footwall imbrication. (c) Salient and recess map pattern and resulting flow, near the thrust, due to warping of the thrust surface.

whatever reason (e.g. slight difference in rock type or geometric orientation of fault), resistance to slip is higher in one area, the footwall may start to deform in this area (cf. Platt and Leggett, 1986; Woodward et al., 1988). As the footwall deforms it is likely to warp the thrust surface, steepening the fault in the region of the slip resistance. This in turn leads to further resistance to slip and the need for more internal deformation. Given the heterogeneous nature of sedimentary packages, it is not surprising that most thrust faults have non-planar geometries. Therefore, we believe that the greater deformation seen within the recess versus the salient (Strine and Mitra, 2004), as well as the non-plane strains observed in this region, are ultimately a result of the non-planar fault geometry.

The local rotation of the flow direction may, too, be related to this warping of the thrust surface. The steepening of the thrust surface was caused by the stacking of footwall imbricates. This stacking created a local gravitational high, which may have undergone collapse during the late stages of deformation. During such a collapse, the spreading direction need not conform with the regional transport direction and may vary significantly between locations. Thus, we propose that gravitational collapse is a possible explanation for the observed late stage change in the flow direction. This collapse hypothesis is supported by the existence of an E–W striking normal fault within this recess (Butler, 1984). An alternative hypothesis is that the emplacement of smaller or 'off-center' imbricate slices could also cause localized variations in flow directions and therefore fold hinge orientations which are oblique to the overall transport direction and mean lineation direction.

6. Conclusions

Strain data from quartzites beneath the Moine thrust and quartz schists above the thrust at Loch Srath nan Aisinnin are consistent with top-to-the-WNW shearing and non-plane strain flattening across the thrust zone. In the footwall, quartzites ranging from 154 to 512 m map distance from the fault trace, *k*-values and *c*-axes textures from deformed relict grains yield data consistent with non-plane strain flattening. Microstructures (e.g. kink bands, asymmetric folds, and asymmetric grain shapes), also, indicate top-to-the-WNW shearing. Footwall samples closer to the thrust ($\geq$19 m) are totally recrystallized. *C*-Axis textures from these samples are consistent with WNW-directed shearing. Moreover, one of these samples has a concentration of *c*-axes subparallel to the *b*-direction consistent with Regime 3 deformation (Hirth and Tullis, 1992). The long axes of the recrystallized grains are subperpendicular to the transport direction, which may be analogous to shearing direction perpendicular lineations seen in transpressional zones (Tikoff and Greene, 1997). Recrystallized quartz grains within quartz-rich layers in the hanging wall Moine Schists also have flattening *k*-values and similar orientations to the footwall relict grains. These flattening *k*-values are consistent with the observed radial fibrous overgrowths seen in the *c*-section. *C*-Axis textures within the hanging wall mylonites are random on the scale of a standard thin-section due to thrust related folding.

We interpret the abundance of general flattening strain data to be a result of non-planar fault geometry. The recess in the fault at this location is due to a footwall imbricate stack, which may have formed as a result of a positive feedback loop between footwall deformation and fault slip resistance. This also explains the relatively high degree to which the footwall rocks have been deformed in this region (Strine and Mitra, 2004) as well as the persistence of the asymmetric *c*-axis textures below the thrust surface. Furthermore, gravitational collapse of this imbricate stack and/or a non-planar internal structure of this stack may explain the observed rotation of the flow direction as seen in the orientations of lineations and foliations when compared with the later fold hinge orientations.

Most numerical models assume plane strain deformation, planar fault surfaces, and an undeformable footwall. However, regions of non-plane strain (such as this one) may have major effects on the overall kinematics of thrust faults; thus, by ignoring them, we undermine our ability to understand the overall kinematics of fold-and-thrust belts.

Acknowledgements

We are indebted to Chuck Bailey, Laurel Goodwin, Rick Law, and Dave Shelley for exceptionally thorough reviews of the present manuscript. We also thank Holger Stunitz at the University of Basel for measuring *c*-axis textures via X-ray goniometry for some of our samples. We gratefully acknowledge both Rick Allmendinger's Stereonet and Neil Mancktelow's StereoPlotXL for help in plotting and contouring stereographic data. Matthew Strine's field work was supported by Geological Society of America Student Research Grants as well as NSF EAR0208001 awarded to G. Mitra. Matthew Strine thanks Stephen McDowall for the many hours he selflessly donated to helping him come up with the best-fit ellipsoid program. And mostly, Matthew thanks his mother, Pam Harrison: "Thanks, Mom". Steve Wojtal thanks Wendy Kozol for her continued support and encouragement.

References

Alsop, G.I., Holdsworth, R.E., 1999. Vergence and facing patterns in large-scale sheath folds. Journal of Structural Geology 21, 1335–1349.

Berthé, D., Choukroune, P., Jegouzo, P., 1979. Orthogneiss, mylonite, and non-coaxial deformation of granite: the example of the South Amorican shear zone. Journal of Structural Geology 1, 31–42.

Borradaile, G.J., 1984. Strain analysis of passive elliptical markers: success of de-straining methods. Journal of Structural Geology 6, 433–437.

Boyer, S.E., 1984. Origin and significance of compositional layering in the

Late Precambrian sediments, Blue Ridge Province, North Carolina, USA. Journal of Structural Geology 6, 121–133.
Boyer, S., Elliott, D., 1982. Thrust systems. Bulletin of American Association of Petroleum Geology 66, 1196–1230.
van Breemen, O., Aftalion, M., Johnson, M.R.W., 1979. Age of the Loch Borrolan complex, Assynt, and late movements along the Moine thrust zone. Journal of the Geological Society of London 136, 89–496.
Butler, R.W.H., 1984. Structural evolution of the Moine thrust belt between Loch More and Glen Dubh, Scotland. Scottish Journal of Geology 20, 161–179.
Carreras, J., Estrada, A., White, S.H., 1977. The effects of folding on the c-axis fabric of a quartz mylonite. Tectonophysics 39, 3–24.
Casey, M., Williams, D., 2000. Micromechanical control of rheological anisotropy in quartz mylonite. Physics and Chemistry of the Earth 25, 127–132.
Chapple, W.M., 1978. Mechanics of thin-skinned fold-and-thrust belts. Geological Society of America Bulletin 81, 1189–1198.
Christie, J.M., 1960. Mylonitic rocks from the Moine Thrust zone between Loch Eriboll and Foinaven, NW Scotland. Transactions of the Edinburgh Geological Society 18, 79–93.
Christie, J.M., 1963. The Moine thrust zone in the Assynt region, NW Scotland. University of California Publication of the Geological Society 40, 345–419.
Cloos, H., 1946. Lineation: a critical review and annotated biography. Geological Society of America Memoir 18.
Cobbold, P.R., Quinquas, H., 1980. Development of sheath folds in shear regimes. Journal of Structural Geology 2, 119–127.
Coward, M.P., 1988. The Moine thrust and the Scottish Caledonides. In: Mitra, G., Wojtal, S. (Eds.), Geometries and Mechanisms of Thrusting, with Special Reference to the Appalachians, Geological Society of America Special Paper, 222., pp. 1–15.
Coward, M.P., Kim, J.H., 1981. Strain within thrust sheets. In: McClay, K.R., Price, N.J. (Eds.), Thrust and Nappe Tectonics. Special Publication—Geological Society of America Memoir 18.
Coward, M.P., Nell, P.R., Talbot, J., 1992. An analysis of the strains associated with the Moine thrust zone, Assynt Northwest Scotland. In: Mitra, S., Fisher, G.W. (Eds.), Structural Geology of Fold and Thrust Belts (the Elliott Volume), Johns Hopkins University Press, pp. 105–122.
Dahlstrom, C.D.A., 1970. Structural geology in the eastern margin of the Canadian Rocky Mountains. Bulletin of Canadian Petroleum Geology 18, 332–406.
Dallmeyer, R.D., Strachan, R.A., Rogers, G., Watt, G.R., Friend, C.R.L., 2001. Dating deformation and cooling in the Caledonian thrust nappes of north Sutherland, Scotland; insights from $^{40}Ar/^{39}Ar$ and Rb–Sr chronology. Journal of the Geological Society of London 158, 501–512.
Davis, D., Suppe, J., Dahlen, F., 1983. Mechanics of fold-and-thrust belts and accretionary wedges. Journal of Geophysical Research. B 88, 1153–1172.
Dell'Angelo, L.N., Tullis, J., 1986. A comparison of quartz c-axis preferred orientations in experimentally deformed aplites and quartzites. Journal of Structural Geology 8, 683–692.
Dell'Angelo, L.N., Tullis, J., 1989. Fabric development in experimentally sheared quartzites. Tectonophysics 169, 1–21.
Durney, D.W., Ramsay, J.G., 1973. Incremental strains measured by syntectonic crystal growth. In: DeJong, K.A., Scholten, R. (Eds.), Gravity and Tectonics, John Wiley, New York, pp. 67–96.
Elliott, D., Johnson, M.R.W., 1980. Structural evolution in the northern part of the Moine thrust belt, NW Scotland. Transactions of the Royal Society of Edinburgh 71, 69–96.
Emerman, S.H., Turcotte, D., 1983. A fluid model for the shape of accretionary wedges. Earth Planetary Science Letters 63, 379–384.
Erickson, S.G., Wiltschko, D.V., 1991. Spatially heterogeneous strength in thrust fault zones. Journal of Geophysical Research 96, 8427–8439.
Evans, D.J., White, S.H., 1984. Microstructural and fabric studies from the rocks of the Moine Nappe, Eriboll, NW Scotland. Journal of Structural Geology 6, 369–389.
Fletcher, R.C., 1989. Approximate analytical solutions for cohesive fold-and-thrust wedge: some results for lateral variations in wedge properties and for finite wedge angle. Journal of Geophysical Research 94, 10, 347–10,354.
Flinn, D., 1962. On folding during three-dimensional progressive deformation. Quarterly Journal of the Geological Society 118, 385–433.
Fossen, H., Tikoff, B., 1993. The deformation matrix for simultaneous pure shear, simple shear, and volume change, and its application to transpression/transtension tectonics. Journal of Structural Geology 15, 413–425.
Freeman, S.R., Butler, R.W.H., Fliff, R.A., Rex, D.C., 1998. Direct dating of mylonite evolution: a multi-disciplinary geochronological study from the Moine thrust zone, NW Scotland. Journal of the Geological Society of London 155, 745–758.
Geiser, P.A., 1988. The role of kinematics in construction and analysis of geological cross sections in deformed terranes. In: Mitra, G., Wojtal, S. (Eds.), Geometries and Mechanisms of Thrusting, with Special Reference to the Appalachians, Geological Society of America Special Paper, 222., pp. 47–76.
Gray, M.B., Mitra, G., 1999. Ramifications of four-dimensional progressive deformation in contractional mountain belts. Journal of Structural Geology 21, 1151–1160.
Handy, M., 1990. The solid-state flow of polymineralic rocks. Journal of Geophysical Research 95, 8647–8661.
Hanmer, S., Passchier, C., 1991. Shear-sense indicators; a review. Geological Survey of Canada Paper 90-17.
Harris, A.L., Johnson, M.R.W., 1991. Moine. In: Craig, G.Y., (Ed.), Geology of Scotland, 3rd ed, Geological Society of London, pp. 87–123.
Hirth, G., Tullis, J., 1992. Dislocation creep regimes in quartz aggregates. Journal of Structural Geology 14, 145–160.
Holdsworth, R.E., 1989. Late brittle deformation in a Caledonian ductile thrust wedge: new evidence for gravitational collapse in the Moine Thrust sheet, Sutherland, Scotland. Tectonophysics 170, 17–28.
Holdsworth, R.E., 1990. Progressive deformation structures associated with ductile thrusts in the Moine Nappe, Sutherland, N. Scotland. Journal of Structural Geology 12, 443–452.
Hongin, F.D., Hippert, J.F., 2001. Quartz crystallographic and morphologic fabrics during folding/transposition in mylonites. Journal of Structural Geology 23, 81–93.
Hossack, J.R., 1967. Pebble deformation and thrusting in the Bygdin Area (southern Norway). Tectonophysics 5, 315–339.
Johnson, M.R.W., 1983. Torridonian–Moine. In: Craig, G.Y., (Ed.), Geology of Scotland, Halsted Press, pp. 49–76.
Johnson, M.R.W., Kelley, S.P., Oliver, G.J.H., Winter, D.A., 1985. Thermal effects and timing of thrusting in the Moine thrust zone. Journal of the Geological Society of London 142, 863–874.
Kelley, S.P., 1988. The relationship between K–Ar mineral ages, mica grain sizes and movement on the Moine thrust zone, NW Highlands, Scotland. Journal of the Geological Society of London 145, 1–10.
Kelley, S.P., Powell, D., 1985. Relationships between marginal thrusting and movement on major, internal shear zones in the Northern Highland Caledonides, Scotland. Journal of Structural Geology 7, 161–174.
Knipe, R.J., Wintsch, R.P., 1985. Heterogeneous deformation, foliation development, and metamorphic processes in a polyphase mylonite. In: Thompson, A.B., Rubie, D.C. (Eds.), Metamorphic Reactions—Kinetics, Textures, and Deformation, Springer-Verlag, New York, pp. 180–210.
LaTour, T.E., 1981. Significance of folds and mylonites at the Grenville front in Ontario: summary. Geological Society of America Bulletin 92, 411–413.
Law, R.D., 1987. Heterogeneous deformation and quartz crystallographic fabric transitions: natural examples from the Moine Thrust zone at the Stack of Glencoul, northern Assynt. Journal of Structural Geology 9, 819–834.
Law, R.D., 1990. fabrics: a selective review of their applications to research

in structural geology. In: Knipe, R.J., Rutter, E.H. (Eds.), Deformation Mechanisms, Rheology and Tectonics, Geological Society Special Publication, 54., pp. 335–352.

Law, R.D., Knipe, R.J., Dayan, H., 1984. Strain path partitioning with thrust sheets; microstructural and petrofabric evidence from the Moine Thrust zone at Loch Eriboll, northwest Scotland. Journal of Structural Geology 6, 477–497.

Law, R.D., Casey, M., Knipe, R.J., 1986. Kinematic and tectonic significance of microstructures and crystallographic fabrics within quartz mylonites from the Assynt and Eriboll regions of the Moine Thrust zone, NW Scotland. Transactions of the Royal Society of Edinburgh, Earth Sciences 77, 99–126.

Lawton, T.F., Sprinkel, D.F., DeCelles, P.G., Mitra, G., Sussman, A.J., Weiss, M.P., 1997. Sevier thrust belt central-Utah: Sevier Desert to Wasatch Paleau. BYU Geology Studies, 33–68.

Lin, S., Jiang, D., 2001. Using along-strike variation in strain and kinematics to define the movement direction of curved transpressional shear zones: an example from northwestern Superior Provicen, Manitoba. Geology 29, 767–770.

Lin, S., Jiang, D., Williams, P.F., 1998. Transpressional (or transtensional) zones of triclinic symmetry: natural example and theoretical modelling. In: Holdsworth, R.E., Strachan, R.A., Dewey, J.F. (Eds.), Continental Transpressional and Transtensional Tectonics, Special Publication of the Geological Society of London, 135., pp. 41–57.

Lisle, R., 1985. Geological Strain Analysis; a Manual for the R_f/ϕ Technique, Pergamon Press, Oxford.

Lister, G.S., 1977. Discussion: cross-girdle c-axis fabrics in quartzites plastically deformed by plane strain and progressive simple shear. Tectonophysics 39, 51–54.

Marshak, S., 1988. Kinematics of orocline and arc formation in thin-skinned orogens. Tectonics 7, 73–86.

McLeish, A., 1971. Strain analysis of deformed Pipe Rock in the Moine Thrust Zone, northwest Scotland. Tectonophysics 12, 469–503.

Means, W.D., 1981. The concept of steady-state foliation. Tectonophysics 78, 179–199.

Means, W.D., Ree, J.-H., 1988. Seven types of subgrain boundaries in octachloropropane. Journal of Structural Geology 10, 765–770.

Mitra, G., 1978. Ductile deformation zones and mylonites; the mechanical processes involved in the deformation of crystalline basement rocks. American Journal of Science 278, 1057–1084.

Mitra, G., 1997. Evolution of salients in a fold-and-thrust belt: the effects of sedimentary basin geometry, strain distribution and critical taper. In: Sengupta, S., (Ed.), Evolution of Geological Structures from Macro- to Micro-scales, Chapman and Hall, London, pp. 59–90.

Mukul, M., Mitra, G., 1998. Finite strain and strain variation analysis in the Sheeprock thrust sheet: an internal thrust sheet in the Provo salient of the Sevier fold-and- thrust belt, Central Utah. Journal of Structural Geology 20, 403–417.

Nadai, A., 1963. Theory of Flow and Fracture of Solids—Engineering Societies Monographs, McGraw-Hill, New York, 705pp.

Newman, J., Mitra, G., 1993. Lateral variations in mylonite zone thickness as influenced by fluid-rock interactions, Linville Falls Fault, North Carolina. Journal of Structural Geology 15, 849–863.

Passchier, C.W., Trouw, R.A.J., 1996. Microtectonics, Springer-Verlag, Berlin.

Peach, B.N., Horne, J., Gunn, W., Clough, C.T., Hinxman, L.W., Teall, J.H.H., 1907. The Geological Structure of the Northwest Highlands of Scotland, Memoir of the Geological Survey of Great Britain, 668pp.

Platt, J.P., Leggett, J.K., 1986. Stratal extension in thrust footwalls, Makram accretionary prism: implications for thrust tectonics. American Association of Petroleum Geologists Bulletin 70, 191–203.

Ramsay, J.G., Huber, M.I., 1983. The Techniques of Modern Structural Geology, vol. 1, Academic Press, London, 462pp.

Ree, J.H., 1991. An experimental steady-state foliation. Journal of Structural Geology 13, 1001–1012.

Ree, J.H., Park, Y., 1997. Static recovery and recrystallization microstructures in sheared octachloropropane. Journal of Structural Geology 19, 1521–1526.

Robin, P.-Y.F., Cruden, A.R., 1994. Strain and vorticity patterns in ideally ductile transpression zones. Journal of Structural Geology 16, 447–466.

Sanderson, D.J., 1982. Models of strain variation in nappes and thrust sheets: a review. Tectonophysics 88, 201–233.

Sanderson, D.J., Marchini, R.D., 1984. Transpression. Journal of Structural Geology 6, 449–458.

Schmid, S., Casey, M., 1986. Complete fabric analysis of some commonly observed quartz c-axis patterns. In: Hobbs, B.E., Heard, H.C. (Eds.), Mineral and Rock Deformation: Laboratory Studies—The Paterson Volume, American Geophysical Union, Geophysical Monograph, 36., pp. 263–286.

Simpson, C., Schmid, S., 1983. An evaluation of criteria to deduce the sense of movement in sheared rock. Geological Society of America Bulletin 94, 1281–1288.

Smart, K.J., Kreig, R.D., Dunne, W.D., 1997. Frictional interplay of two thrust flats: insights from finite element analyses. Geological Society of America Abstracts with Programs 29/6, A44.

Smart, K.J., Kreig, R.D., Dunne, W.D., 1999. Deformation behavior during blind thrust translation as a function of fault strength. Journal of Structural Geology 21, 855–874.

Starkey, J., Cutforth, C., 1978. A demonstration of the interdependence of the degree of quartz preferred orientation and the quartz content of deformed rocks. Canadian Journal of Earth Sciences 15, 841–847.

Strayer, L.M., Hudleston, P.J., 1997. Simultaneous folding and faulting and fold-thrust belt evolution: a distinct element model. Geological Society of America Abstracts with Programs 29/6, A44.

Strayer, L.M., Hudleston, P.J., 1998. Controls of duplex formation: results from numerical models. Geological Society of America Abstracts with Programs 30/7, A42.

Strine, M., Mitra, G, 2004. Preliminary kinematic data from a salient-recess pair along the Moine thrust, NW Scotland. Ed. Sussman, A. and Weil, A. Geological Society of America Special Paper, in press.

Tikoff, B., Greene, D., 1997. Stretching lineations in transpressional shear zones. Journal of Structural Geology 19, 29–40.

Tullis, J., Heilbronner, R., 2002. Microstructural evolution in quartzites experimentally deformed to high shear strains. Geological Society of America Abstract with Programs 34/6, 39.

Tullis, J., Wenk, H.-R., 1994. Effect of muscovite on the strength and lattice preferred orientations of experimentally deformed quartz aggregates. Materials Science and Engineering A175, 209–220.

Twiss, R.J., Unruh, J.R., 1998. Analysis of fault-slip inversions: do they constrain stress or strain rate. Journal of Geophysical Research 103, 12, 205–12,222.

Twiss, R.J., Protzman, G.M., Hurst, S.D., 1991. Theory of slickenline patterns based on the velocity gradient tensor and microrotation. Tectonophysics 186, 215–239.

White, S.H., Evans, D.J., Zhong, D.L., 1982. Fault rocks of the Moine thrust zone; microstructures and textures of selected mylonites. Textures and Microstructures 5, 33–61.

Wilkinson, P., Soper, N.J., Bell, A.M., 1975. Skolithos pipes as strain markers in mylonites. Tectonophysics 28, 143–157.

Wojtal, S.F., 1986. Deformation within foreland thrust sheets by populations of minor faults. Journal of Structural Geology 8, 341–360.

Wojtal, S.F., 2001. The nature and origin of asymmetric arrays of slip surfaces in fault zones. In: Holdsworth, R.E., Strachan, R.A., Magloughlin, J.R., Knipe, R.J. (Eds.), The Nature and Tectonic Significance of Fault Zone Weakening, Special Publication of the Geological Society of London, 186., pp. 171–193.

Wojtal, S., Mitra, G., 1988. Nature of deformation in fault rocks from Appalachian thrusts. In: Mitra, G., Wojtal, S. (Eds.), Geometries and Mechanisms of Thrusting, with Special Reference to the Appalachians, Geological Society of America Special Paper, 222., pp. 17–33.

Woodward, N.B., Wojtal, S., Paul, J.B., Zadins, Z., 1988. Partitioning of deformation within several external thrust zones of the Appalachian orogen. Journal of Geology 96, 351–361.